ACING VERSATILITY OF RIS PARTITIONING: AN EXPERIMENTAL PROOF-OF-CONCEPT CAMPAIGN

Ahmed Nasser , Abdulkadir Celik , Asmaa Abdallah , Ruiqi Wang , Yiming Yang , Atif Shamim , and Ahmed M. Eltawil

ABSTRACT

Reconfigurable Intelligent Surfaces (RIS) have emerged as an innovative technology for enhancing signal reception by manipulating the channel state and enabling passive beamforming toward targeted directions. Nonetheless, the effective deployment of RIS relies on precise phase shift optimization, a challenge exacerbated by restricted computational resources and the need for accurate channel state information. In this context, predefined codebooks and RIS partitioning deployment offer strategic solutions, enabling the RIS to serve multiple users simultaneously by assigning different partitions to various tasks and selecting the optimal codeword for specific objectives. As efforts to standardize RIS, this article presents an experimental testbed developed to assess the impact of RIS partitioning in the millimeter-wave band across several scenarios, including enhancing data rates in grant-free non-orthogonal multiple access, managing interference in heterogeneous networks, and maximizing secrecy capacity in physical layer security contexts. By investigating these case studies, this article provides empirical insights into the versatility and effectiveness of RIS partitioning across various communication environments. The research concludes by discussing the crucial challenges in RIS hardware design and implementation, emphasizing innovative pathways for advancing RIS technology in wireless infrastructures.

INTRODUCTION

Reconfigurable intelligent surfaces (RIS) has introduced a revolutionary technology for augmenting spectral and energy efficiency, coverage, and security of wireless networks, providing solutions for the urgent need for high data rates across diverse services provided by the next generations of wireless networks. RIS is engineered as an array of passive, low-power, and electronically adjustable meta-surface elements that can modify electromagnetic properties of incident radio frequency (RF) signals to perform various functionalities such as reflection, refraction, polarization, absorption, etc [1]. In particular, reflection can be realized through optimal amplitude and phase shift of RIS elements to enable passive beamforming that

can substantially improve the channel quality and signal reception by maximizing the channel gain towards a direction of interest—all without the unwanted noise typically amplified by conventional amplify-and-forward relays. With its innovative features, RIS heralds the concept of "environment-as-a-service" by providing a degree of control over the wireless environment and paves the way for versatile solutions to various persistent problems in wireless communication such as blockage overtake, interference management, physical layer security, localization, and coverage extension, to name a few [2].

The effective deployment of RIS hinges on the precise optimization of phase shifts, without which passive beamforming gain may experience significant degradation or beam misalignment may cause interference, leading to a degradation in the overall achieved data rate. The optimal phase shift configuration necessitates the availability of channel state information (CSI) for all network entities. However, considering the cost-effective and energy-efficient design criteria inherent to RIS, the limited computational resources at the RIS complicate the estimation of channels, especially as the number of RIS elements-and thereby the channel dimensions-increases [3]. Furthermore, acquiring CSI at the transceiver side introduces additional challenges, owing to the complex cascaded channel traversing the RIS. Even if accurate CSI is available, achieving optimal phase shifts in practical RIS applications are often subject to quantization granularity, which is primarily responsible for quantization errors and sidelobe power, inadvertently strengthening the channel link in undesirable directions. Moreover, phase shift discretization turns optimal RIS configuration into a combinatorial and often non-convex optimization problem, solution of which is computationally prohibitive even for a moderate size of RIS.

One strategy to overtake the need for CSI acquisition involves selecting reflective beams from predefined codebooks, such as the generic discrete Fourier transform (DFT) or site-specific codebooks [4]. While effective in the absence of CSI, this method typically directs the signal in a single direction, restricting the RIS's utility to serving only one user equipment (UE) or a group of UEs located in the same direction. A promising

Ahmed Nasser (corresponding author), Asmaa Abdallah, Ruiqi Wang, Yiming Yang, Atif Shamim, and Ahmed M. Eltawil are with the Computer, Electrical, and Mathematical Sciences and Engineering (CEMSE) Division, King Abdullah University of Science and Technology (KAUST), Thuwal 23955-6900, Kingdom of Saudi Arabia; Abdulkadir Celik is with the School of Electronics and Computer Science, University of Southampton, SO17 1BJ Southampton, U.K.

Digital Object Identifier: 10.1109/MCOMSTD.2025.3608130

solution recently gaining attention is the RIS partitioning approach that virtually divides the RIS into multiple partitions, with each partition's phase shifts set to different beams from the codebook, thus enabling the RIS to enhance or attenuate multiple paths and offer diverse functionalities [5], [6]. The scarcity of practical experimental studies assessing RIS partitioning across various scenarios underscores the importance of this article's contributions.

In this article, we introduce an experimental testbed developed to evaluate the performance of RIS partitioning in millimeter wave (mmWave) band across various scenarios. We analyze data collected from this testbed through three distinct case studies, each aimed at different objectives: 1) enhancing data rates in grant-free (GF) non-orthogonal multiple access (NOMA), 2) interference management in heterogeneous networks (HetNets), and 3) maximizing secrecy capacity (SC) in physical layer security (PLS). The results provided by these case studies offer diverse experimental insights into the effectiveness of RIS partitioning from multiple perspectives, offering meaningful contributions to RIS standardization efforts. The article concludes by pinpointing key hurdles in RIS hardware design and implementation, suggesting potential solutions for future directions.

EXPERIMENTAL SETUP AND MEASUREMENT CAMPAIGN

The proposed setup facilitates experimentation and data collection required for evaluating the RIS-partitioning approach across various scenarios within the mmWave spectrum. The specifics of the setup configuration are shown in Fig. 1 and detailed as follows:

 RIS: The RIS array utilized operates within the mmWave 5G n257 and n258 bands, comprising 400 elements arranged in a 20×20 grid. The array occupies a total area measuring

- 77×77 mm², equivalent to 7.1 λ ×7.1 λ , with λ defining the free-space wavelength at 27.5 GHz. Each element's phase configuration employs a 1-bit discretized phase distribution, enabling two-phase states (i.e., on-off phases) controlled by a p-i-n diode affixed to each element. These phase states vary with frequency, necessitating an optimal ON/OFF pattern tailored to the incident frequency under constant environmental and design conditions. An ESP-WROOM-32 module handles control over the entire RIS, overseeing serial communication for UE interaction and computing array patterns to bias the 400 p-i-n switches. Further details on the design and fabrication of the utilized RIS can be found in [7]
- **BS:** The BS is equipped with a highly directional PE9851B/SF-20 transmitting horn antenna, featuring a WR-34 rectangular waveguide interface designed for operation in the 22-33 GHz frequency range and offering a nominal gain of 20 dBi. This high directivity enables the transmitter to effectively focus energy in specific directions, such as toward the UE or RIS, mimicking a beamforming-like behavior without the need for digital or analog phased-array beamforming. The BS is located at a distance of approximately d_{BS} = 3m away and at an angle of $\theta_{BS} = -30^{\circ}$ from the RIS to guarantee that a plane wave reaches the RIS. A Keysight VXG M9384B signal generator is connected to the horn antenna, delivering a continuous wave signal with adjustable output power ranging from -10 dBm to 20 dBm.
- **UEs:** UEs are equipped with a PE9851B/ SF-20 receiving horn antenna, similar to that of the BS. They are connected to a USRB x310 equipped with two 40MHz UBX daughterboards and a Xilinx Kintex-7 FPGA. The USRB is further linked to two TMYTEK development down-converter

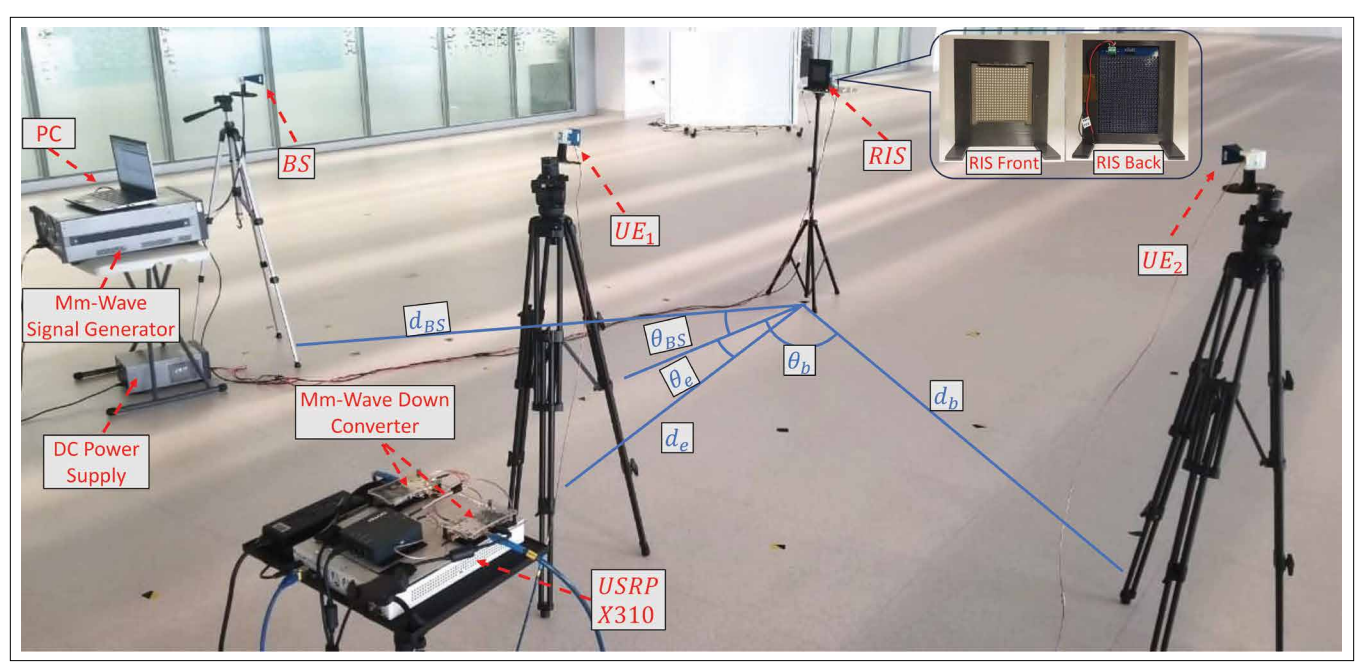


FIGURE 1. The photograph of the experimental setup for RIS case studies.

boards, which down-convert signals from the mmWave range received by the antenna to a 6GHz signal compatible with the USRB. A workstation laptop is connected to the USRB via a 1GB Ethernet cable for signal processing. While collecting received signal strength indicator (RSSI) datasets, UE₁ and UE₂ are positioned at various locations within the RIS coverage area, with distances d_1 and d_2 ranging from 3 to 6 meters from the RIS, to ensure that both UEs are in the far-field region. This placement satisfies the condition of being beyond the Rayleigh distance, which is approximately 2.2 meters based on the RIS dimensions and operating frequency, as calculated in [7]. In addition, UE₁ spans angles θ_1 ranging from 0° to 40°, while UE₂ spans angles θ_2 ranging from 45° to 70°, measured relative to the RIS.

The workstation laptop functions as a central unit, linking all the testbed components, managing control signaling, and facilitating both synchronization and signal processing across the entire system. The transceivers operates at a carrier frequency of $f_c = 28$ GHz. As discussed in [6], the number of RIS partitions should be less than or equal to the number of UEs. In this study, we limit our implementation to two users and a maximum of two RIS partitions (i.e., top and bottom), as this is sufficient to demonstrate the primary objective of this work. This setup allows us to thoroughly analyze and provide a proof-ofconcept for RIS partitioning in practical scenarios without introducing unnecessary complexity. The conducted numerical results in the following section compare two approaches: 1) Full RIS beam sweeping and 2) RIS partitioning beam sweeping. In the Full RIS beam sweeping approach, the RIS sweeps through a specially designed angle-based codebook containing 90 beams, each directing incident signals toward angles ranging from 0 to $\pi/2$. Each beam consists of 400 phase shifts corresponding to the full RIS elements with a 1-bit quantized phase resolution. The detailed codebook design can be found in [7]. In contrast, the RIS partitioning beam sweeping approach divides the RIS virtually into two equal partitions. Two beams are simultaneously selected from a codebook of 90 beams, one for each partition, resulting in a sweep over 902 possible combinations. Each beam in the RIS partitioning codebook consists of 200 phase shifts, corresponding to half of the RIS elements. In this study, we focus on equal RIS partitioning, as it serves as a benchmark for evaluating the performance of the RIS partitioning approach. Furthermore, neither the CSI nor the UEs' positions are known to the BS in this study. In the rest of the paper, we will utilize the RSSI dataset collected by the two UEs in the proposed testbed shown in Fig. 1 to evaluate the effectiveness of the RIS-partitioning approach across various case studies.

GRANT-FREE NON-ORTHOGONAL MULTIPLE ACCESS

Power-domain NOMA (PD-NOMA) boosts spectral efficiency by allowing multiple UEs to share the same network resources at varying power levels, enabling the use of successive interference cancellation (SIC) at the receiver. Nevertheless, PD-NOMA gain depends crucially on power

reception disparity among UEs; without which inter-cluster interference intensifies [8]. However, PD-NOMA has limited scalability due to the grant-acquisition and power control requirements, especially for uplink transmission. In this case, UEs first need to coordinate with the BS to be granted access for RBs, then exchange CSI information to perform optimal power control. At this point, RIS partitioning introduce an "over-the-air" power control by manipulating the channel gain disparity among UEs, thereby eliminating the need for power control at UE side and facilitating a grant-free NOMA scheme.

Nonetheless, GF-NOMA still requires the BS to acquire the cascaded CSI for efficient operation and coordination with the RIS [9]. Alternatively, we adopt a beam selection strategy to optimize RIS phase shifts, aiming to maximize channel disparity among UEs. While this approach can potentially increase the overall spectral efficiency of PD-NOMA, it might not meet the required QoS for all UEs or ensure fairness, as the beam selection may favor UEs with superior channel conditions. Fortunately, RIS-partitioning can be a viable solution by configuring each partition to enhance the channel for a specific path, preserving the necessary channel disparities, and allowing the use of fixed power allocation while satisfying QoS requirements. However, this approach complicates beam selection due to the need to choose a specific beam for each partition, thereby increasing the complexity of the selection process and necessitating more sophisticated selection algorithms. Additionally, partitioning can lead to reduced beamforming gain, as the available elements are divided among multiple partitions instead of being used collectively.

In this case study, we aim to validate the effectiveness of RIS partitioning within the GF-NOMA framework, where neither the CSI nor the positions of the UEs are known to the BS. As shown in Fig. 2 (leftmost), a BS operating in the mmWave band dispatches two superimposed signals to serve two single-antenna UEs, with the aid of the RIS, despite obstructed LoS paths between the BS and the UEs. While our testbed employs a single horn antenna at both the BS and UE sides, the multiple beams shown in Fig. 2 (leftmost) are intended to represent the possible logical communication links between the BS, RIS, and UEs, rather than the actual radiation patterns of the antennas, indicating that the direct path between the BS and UEs is blocked. The RIS is virtually equi-partitioned, and each is pre-assigned to a specific UE. A fixed power allocation strategy is employed, where 25% of the transmit power, P_t , is allocated to whichever UE has the higher RSSI value. This use case is experimentally evaluated using the setup shown in Fig. 1, where UE₁ and UE₂ in Fig. 2 correspond to the same UE₁ and UE₂ depicted in the experimental setup of Fig. 1.

The performance of this use case is evaluated in Fig. 2 through beam sweeping across the codebook to maximize the combined rate of UE_1 and UE_2 while maintaining a fairness constraint. Fig. 2 (middle) examines the individual rates of UE_1 and UE_2 , along with the total achievable rate at different P_t . It is shown that RIS partitioning yields a modest improvement, not exceeding 10% over the full RIS scenario, which is expected given that

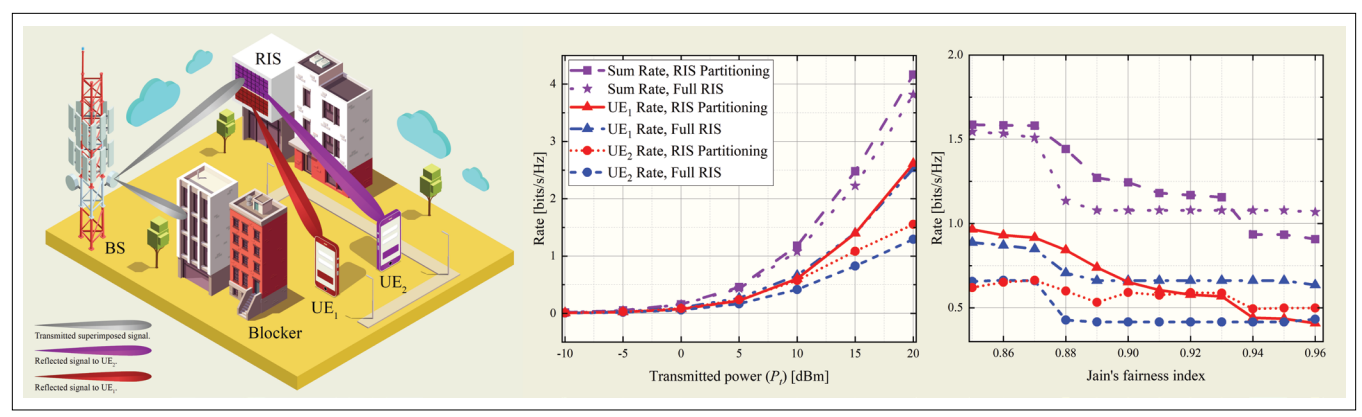


FIGURE 2. The performance evaluation for RIS partitioning in the context of GF-NOMA framework.

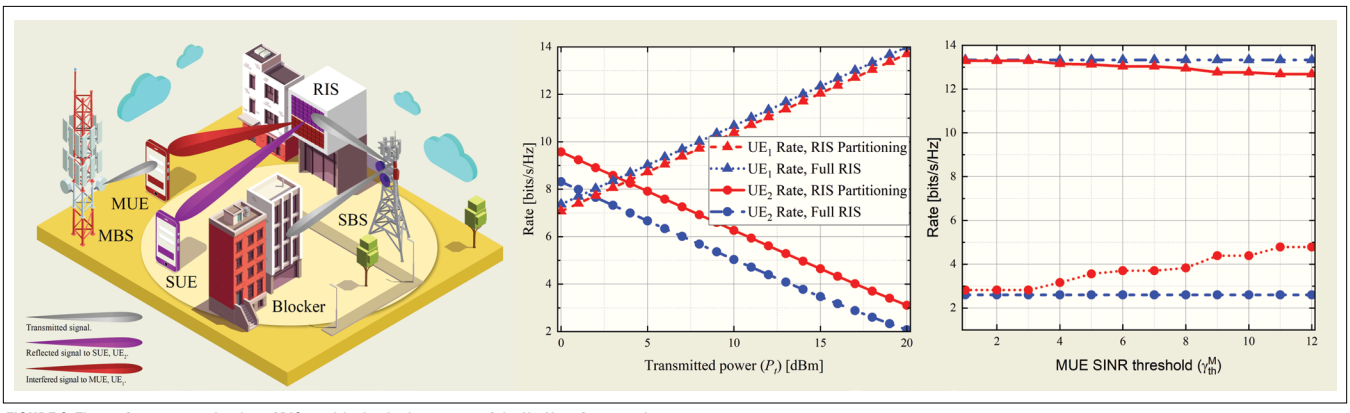


FIGURE 3. The performance evaluation of RIS partitioning in the context of the HetNets framework.

the total reflected power remains constant. However, the primary advantage of RIS partitioning lies in how it distributes the reflected power in various directions to satisfy fairness or QoS constraints among UEs. For example, at $P_t = 15$ dBm, the full RIS results in a rate difference of 0.6 bits/s/Hz between the two UEs, whereas RIS partitioning reduces this difference to 0.3 bits/s/Hz. To delve deeper into this aspect, we analyze the rates for UE₁ and UE₂ against different thresholds of Jain's fairness index, as illustrated in Fig. 2 (rightmost). Increasing the fairness threshold generally leads to a reduction in the achievable rate, since optimal fairness does not necessarily coincide with the highest rate. Nonetheless, RIS partitioning demonstrates a capability to maintain a reasonable total rate while adhering to stringent fairness requirements. In contrast, the full RIS setup cannot keep up with these enhanced fairness demands and tends to reach a point of performance saturation.

INTERFERENCE MANAGEMENT IN HETNETS

Cell densification is a commonly practiced approach to enhance spectrum efficiency, coverage, and connectivity, especially in densely populated regions. In particular, HetNets is formed by overlaying small BSs (SBSs) on the macro BS (MBS) coverage area, allowing SBSs to share available network resources while alleviating congestion by offloading traffic from MBS. One of the pivotal challenges in HetNets is the mitigation of cross-tier interference, which occurs between cells of varying sizes and power outputs [10].

Conventional methods for mitigating interference in HetNets demand acquisition and exchange of the CSI for UEs associated with SBSs and MBSs, which are referred to as small UEs (SUEs) and macro UEs (MUEs), respectively. This requirement dramatically complicates the interference mitigation process and consumes substantial network resources, often proving impractical in real-world scenarios. Recently, RIS has shown its ability to effectively manage interference within HetNets, provided their phase shifts are correctly optimized; otherwise, the interference can exacerbate [11].

As depicted in Fig. 3 (leftmost), we conceptualize a beam selection strategy for RIS-aided HetNets, wherein a specific beam can be assigned to reflect the signal from a SBS toward a cell-edge or obstructed SUE, enhancing its channel link quality and achievable data rate. However, the beam reflected signal towards SUE may substantially degrade the performance of a cell-edge MUE due to the amplified cross-tier interference. A viable solution is to implement a RIS-partitioning strategy, where one partition improves the channel path for the cell-edge SUE to meet QoS requirements whereas the other partition reduces interference affecting the MUE by keeping it below a certain threshold. Accordingly, this use case evaluates the effectiveness of RIS partitioning within the HetNets framework. In Fig. 3 (leftmost), a single-antenna SBS in the mmWave band serves an obstructed SUE with support from a RIS. Meanwhile, a single-antenna MUE at the edge of the small cell experiences interference caused by the RIS-reflected signal. The SBS, SUE, and MUE correspond to the BS, UE₁, and UE₂, respectively, in the experimental setup shown in Fig. 1. The phase shifts of RIS equi-partitions are tailored either to boost the data rates for the SUE or to mitigate interference impacting the MUE.

By conducting beam sweeping across the codebook to maximize the sum rate of SUE and MUE while adhering to QoS constraints for both UEs, Fig. 3 (middle) explores the achievable rates for SUE and MUE at varying SBS's power, P_t . Typically, increasing the SBS's power boosts the rate for SUE but reduces MUE's rate due to heightened cross-tier interference. However, the result demonstrates that RIS partitioning can enhance the rate for MUE by about 25% compared to full RIS configurations by minimizing cross-tier interference, with a negligible reduction of less than 1% in SUE's rate. Additionally, Fig. 3 (rightmost) illustrates the achievable rates for SUE and MUE under various SINR constraints for the MUE, γ_{th}^{M} . Increasing γ_{th}^{M} for the MUE necessitates a reduction in cross-tier interference, thereby improving its rate. The result shows that the RIS-partitioning scenario significantly boosts the MUE rate as the SINR increases, while the full RIS setup struggles to meet these heightened SINR demands and experiences performance saturation. For instance, at an SINR of $\gamma_{th}^{M} = 0.5$, RIS partitioning can enhance the MUE rate by 55% compared to the full RIS configuration, with only a minimal reduction in the SUE rate of less than 2%. These results demonstrate the adaptive functionality of each partition in the RIS-partitioning scenario.

PHYSICAL LAYER SECURITY

The inherent broadcast nature of wireless channels, along with the extended coverage offered by emerging wireless technologies, increases the susceptibility of UEs to attacks from eavesdroppers or malicious devices, making it easier to intercept private communications between legitimate UEs. A viable approach to address these security challenges involves the implementation of PLS in higher layers, improving the security of data links by exploiting the inherent randomness of wireless channels [12]. Recently, RIS has been integrated into PLS frameworks to enhance security by focusing signals toward the legitimate UE, achieved through RIS phase shift optimization.

Although optimizing the full RIS phase shifts via beam selection can significantly enhance the data rate for the legitimate UE, it may not adequately address the direct BS-to-eavesdropper link, potentially allowing eavesdroppers to decode sensitive data. Furthermore, the sidelobes generated by quantization errors stemming from the discretization of phase shifts could unintentionally enhance the eavesdropper's channel link, compromising the security. Partitioning the RIS and superimposing sensitive data with artificial noise (AN) offers a promising solution. RIS partitions can be configured to enhance the legitimate UE's signal while amplifying AN toward eavesdroppers, thereby boosting the overall SC (i.e., the difference between the legitimate UE's rate and the eavesdropper rate) [5], [6].

In this use case, we explore a secure wireless communication strategy where a single-antenna BS securely transmits data to a legitimate UE in the presence of an eavesdropping UE, with RISassisted mitigation, as depicted in Fig. 4 (leftmost). The BS transmits two mmWave superimposed signals: the desired signal and the AN. The RIS is divided into two equal partitions: one enhances the private message, and the other intensifies the jamming impact of AN. The AN is composed of a pseudo-random noise (PRN) sequence, the seed and parameters of which are known only to the legitimate UE, allowing the legitimate UE to cancel out the AN before the decoding process. The power allocation between the AN and the useful signal is critical for enhancing the overall SC. Hence, a power allocation factor, $\alpha \in [0, 1]$, is employed to specify the proportion of the BS's power dedicated to data transmission, with the remaining transmit power, $(1-\alpha)P_t$, allocated to the AN. The PLS use case is explored experimentally using the setup depicted in Fig. 1, wherein UE₂ represents the legitimate UE and UE₁ acts as the eavesdropper.

Performance comparisons between RIS-partitioning and full RIS scenarios are depicted in Fig. 4. Here, a beam-sweeping technique is applied across the utilized codebook to maximize the SC while maintaining the quality of service (QoS) constraints for UE₂ and ensuring that UE₁ 'SINR is below a predetermined threshold that limit maximum data sniffing. In Fig. 4 (middle), the achievable rates for the legitimate UE₂ and the eavesdropping UE₁, as well as the SC across

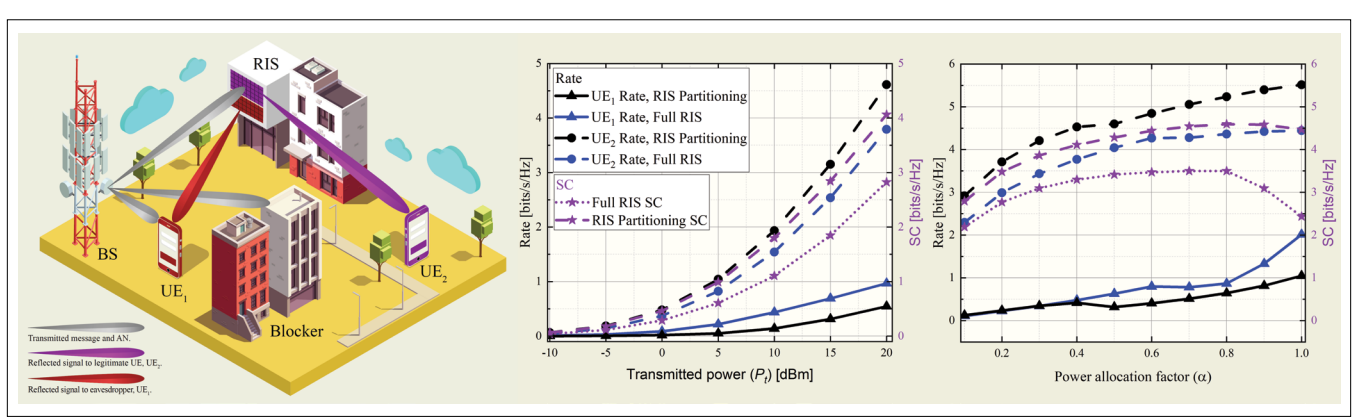


FIGURE 4. The performance evaluation of RIS partitioning in the context of PLS framework.

FIGURE 5. Illustration of the radiation patterns for a full RIS and a two-partition RIS under different quantization levels: ideal continuous phase shift, 1-bit, and 2-bit quantization, with the transmitter positioned at -30°.

various transmission power levels, P_{tr} for $\alpha = 0.8$, are evaluated. The findings indicate that RIS partitioning typically improves SC by about 55% compared to the full RIS setup. This enhancement in SC can be attributed to RIS partitioning boosting the rate for UE₂ by roughly 25% by amplifying the intended signal and simultaneously suppressing UE₁ rate by 30% by intensifying the AN directed at the eavesdropper. This effectively highlights the distinct roles of the two selected beams in the RIS partitioning scenario.

Moreover, Fig. 4 (rightmost) assesses the achievable rates and the SC using different power allocation factors α . This analysis illustrates that although allocating a portion of the BS's power to transmit AN might slightly reduce the rate available to the intended UE₂, it significantly boosts the SC and limits the amount of data that eavesdropper UE₁ can decode by diminishing its SINR. However, it is evident that while the full RIS scenario requires at least 30% of the total power to be allocated to AN to achieve its maximum SC, the RIS-partitioning scenario only needs 10% of the total power to reach its maximum SC, demonstrating the superior efficacy of the RIS-partitioning approach.

HARDWARE IMPAIRMENTS AND POTENTIAL REMEDIES

The literature contains limited reported works on RIS hardware, particularly for operations extending into the mmWave range. The authors of this work have proposed two state-of-the-art wideband RIS hardware designs tailored for 5G mmWave communications, including the design utilized in this study [7] and another recently proposed model [13]. However, numerous unresolved issues persist within RIS hardware development, presenting many potential directions for future research. In this context, we have outlined several insights into RIS hardware as follows.

2-bit Phase-Quantized RIS: In practical RIS implementations, phase shift discretization is essential but turns the phase optimization into a combinatorial challenge, even for moderately sized RIS. Reducing quantization granularity can relax complexity but degrades beamforming by introducing high sidelobes. Additionally, while RIS partitioning enables multipath control and diverse

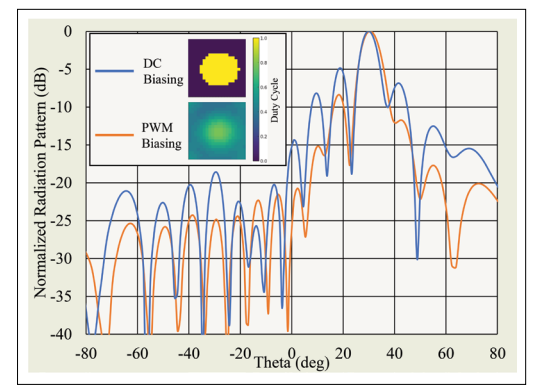


FIGURE 6. Simulated radiation pattern of the RIS with DC and PWM biasing.

functionalities, it compromises beamforming gain by distributing elements across partitions. Fig. 5 illustrates the radiation patterns for a full RIS and a two-partition RIS under different quantization levels: ideal continuous phase shift, 1-bit, and 2-bit quantization. With the transmitter positioned at -30°, the full RIS is configured to reflect the signal toward 0°, while in the partitioned RIS case, each partition is configured with a codeword selected to steer reflections toward 0° and 30°, respectively. Fig. 5 shows that higher quantization granularity reduces sidelobes and improves beamforming gain in the desired direction. Even though exploiting varactor diodes can realize continuous phase control in unit cells, capacitance tuning range limitations at higher frequencies constrain the phase variation range and the operational bandwidth. Considering the loss for 1-bit, 2-bit, and 3-bit phase quantization is 3 dB, 0.6 dB, and 0.2 dB, respectively [14], a 2-bit phase-quantized RIS designs should be a promising trade-off solution for suppressing the side lobe levels while maintaining an acceptable design complexity.

Time-Modulated RIS: While it is acknowledged that improving quantization granularity significantly mitigates sidelobes and quantization lobes, doubling the number of bits for each unit cell proportionally escalates the number of required switches, thereby increasing costs and complexities in hardware implementations. To enhance the reconfigurability of 1-bit RIS without increasing the switch count, time modulation—specifically pulse-width modulation (PWM) biasing-has been proposed as an alternative strategy. By adjusting the duty cycle, the RIS unit cells alternate between ON and OFF states, with the reflection coefficient representing the weighted average of these states when measured at the fundamental frequency of the modulated reflection [15]. Consequently, modifying the duty cycles of the PWM biasing on unit cells introduces additional flexibility in the reflection magnitude distribution, facilitating amplitude tapering and sidelobe suppression. The simulated radiation pattern in Fig. 6 shows that employing PWM biasing at 29.5 GHz with the feed antenna positioned 30 cm away and -30° from the RIS leads to a significant reduction in sidelobe power, approximately 5 dB, attributed to the effects of magnitude tapering with PWM biasing.

On-Chip/On-Wafer RIS for Sub-TeraHertz (THz) Operations: 6G networks are anticipated to operate at sub-THz frequencies (~ 100 GHz), wherein conventional printed circuit board (PCB) technologies struggle to meet the high-resolution requirements and face formidable challenges to integrate minuscule unit cells of sub-THz RISs. In contrast, advancements in Silicon (Si) technology has made substantial strides in achieving high resolution, integration of electronics with electromagnetic (EM) structures, repeatability, reliability, and robustness, making Si-based micro and nano-fabrication processes ideally suited for developing sub-THz RIS systems. However, the monetary implications of manufacturing a large RIS chip using the latest complementary metal-oxide-semiconductor (CMOS) processes remain a considerable hurdle. A promising alternative involves utilizing a CMOS-compatible process that employs phase change materials, such as vanadium dioxide (VO2), for high-frequency switching instead of relying on high-frequency transistors that necessitate more sophisticated CMOS processes. This approach enables reconfiguration through thin film VO2 switches that are compatible with the back end of line (BEOL) of the CMOS process, providing a cost-effective and technically feasible solution for the next generation of RIS technology [13].

CONCLUSION AND FUTURE DIRECTIONS

Contributing to ongoing RIS standardization efforts, we have demonstrated in this article an experimental proof-of-concept for RIS partitioning across three prominent mmWave scenarios, showcasing its adaptability and effectiveness in diverse communication environments. The partitioning in GF-NOMA scenarios efficiently distributes reflected power, upholds channel disparities, and achieves fairness and QoS demands. In HetNets, RIS partitioning mitigates cross-tier interference at the MUEs, satisfying higher SINR requirements while minimally impacting the SUE's rate. Moreover, RIS partitioning augments PLS by boosting the desired signals of legitimate users and diminishing the eavesdropper's rate through targeted AN. We outline the future enhancements planned for our testbed, which are pivotal for elevating its applicability and performance in real-world

- Deploying MIMO Antennas at UE Side:
 While the current static setup is suitable for
 the fixed BS and RIS positions, it poses chal lenges in real-world scenarios where mobile
 UEs are often unaware of the RIS position.
 Substituting horn antennas with MIMO phased arrays will empower UEs to perform
 beamforming independently, determining
 the optimal path to the RIS while concurrently optimizing the RIS's phase shifts.
- RIS-Aided ISAC: Incorporating diverse sensing modalities such as cameras, LiDAR, and radar facilitates the capture of crucial data, including UEs' position, angle, and distance. Hence, integrated sensing and communication (ISAC) can foster the development of deep learning-based beam selection techniques, crucial for optimizing communications in dynamic environments and enabling

adaptive beamforming strategies that can adjust in real-time to changes in UE positions and wireless environment. RIS can also be used for sensing over non-line-of-sight (NLoS) channels, facilitating improvement in situational awareness and safety. Further research is needed to optimize RIS configurations for effective NLoS sensing, exploring different deployment scenarios and enhancing detection accuracy and reliability.

- RIS-Assisted Near-Field Communications:
 Future research should focus on the impact of RIS assistance in near-field communication, necessitating a reevaluation of codebook designs, including those based on sub-array or partitioning strategies. Additionally, dynamic RIS configurations can adjust near-field and far-field regions by switching RIS elements or partitions on and off to modify the aperture size. Leveraging adjustable near-field and far-field regions in dynamic RIS configurations allows for a balanced tradeoff between performance and complexity, presenting an intriguing avenue for future research.
- RIS-Aided Full-Duplex Communication: RIS
 partitions can be arranged to meet QoS
 demands for both uplink and downlink UEs.
 By assigning different RIS partitions to handle UL and DL traffic distinctly, interference
 between these channels can be minimized,
 optimizing resource allocation and improving overall system efficiency. This approach
 ensures that UL and DL transmissions do not
 degrade each other's performance, leading
 to improved overall system efficiency.

REFERENCES

- [1] Y. Liu et al., "Reconfigurable intelligent surfaces: Principles and opportunities," *IEEE Commun. Surveys Tuts.*, vol. 23, no. 3, pp. 1546–1577, 3rd Quart., 2021.
- [2] A. Magbool et al., "Multi-functional RIS for a multi-functional system: Integrating sensing, communication, and wireless power transfer," *IEEE Netw.*, vol. 39, no. 1, pp. 71–79, Jan. 2025
- [3] L. Wei et al., "Channel estimation for RIS-empowered multi-user MISO wireless communications," *IEEE Trans. Commun.*, vol. 69, no. 6, pp. 4144–4157, Jun. 2021.
 [4] A. Abdallah et al., "Multi-agent deep reinforcement learn-
- [4] A. Abdallah et al., "Multi-agent deep reinforcement learning for beam codebook design in RIS-aided systems," *IEEE Trans. Wireless Commun.*, vol. 23, no. 7, pp. 7983–7999, Jul. 2024.
- [5] S. Arzykulov et al., "Artificial noise and RIS-aided physical layer security: Optimal RIS partitioning and power control," *IEEE Wireless Commun. Lett.*, vol. 12, no. 6, pp. 992–996, Mar. 2023.
- [6] S. Arzykulov et al., "Aerial RIS-aided physical layer security: Optimal deployment and partitioning," *IEEE Trans. Cognit. Commun. Netw.*, vol. 10, no. 5, pp. 1867–1882, Oct. 2024.
- [7] R. Wang et al., "A wideband reconfigurable intelligent surface for 5G millimeter-wave applications," IEEE Trans. Antennas Propag., vol. 72, no. 3, pp. 2399–2410, Mar. 2024.
- [8] A. Nasser et al., "Rendezvous of ISAC and NOMA: Progress and prospects of next-generation multiple access," IEEE Commun. Standards Mag., vol. 8, no. 2, pp. 44–51, Jun. 2024
- [9] M. Makin et al., "Optimal RIS partitioning and power control for bidirectional NOMA networks," *IEEE Trans. Wireless Commun.*, vol. 23, no. 4, pp. 3175–3189, Apr. 2024.
- Commun., vol. 23, no. 4, pp. 3175–3189, Apr. 2024. [10] A. Nasser et al., "Data-driven spectrum allocation and power control for NOMA HetNets," *IEEE Trans. Veh. Technol.*, vol. 72, no. 9, pp. 11685–11697, Apr. 2023.
- [11] X. Mu et al., "Intelligent reflecting surface enhanced multi-UAV NOMA networks," *IEEE J. Sel. Areas Commun.*, vol. 39, no. 10, pp. 3051–3066, Oct. 2021.
- [12] N. Wang et al., "Physical-layer security of 5G wireless networks for IoT: Challenges and opportunities," *IEEE Internet Things J.*, vol. 6, no. 5, pp. 8169–8181, Oct. 2019.

- [13] Y. Yang et al., "A fully screen-printed vanadium-dioxide switches based wideband reconfigurable intelligent surface for 5G bands," 2024, arXiv:2404.19646.
- [14] H. Yang et al., "A study of phase quantization effects for reconfigurable reflectarray antennas," *IEEE Antennas Wireless Propag. Lett.*, vol. 16, pp. 302–305, 2017.
 [15] X. Cao et al., "A 1-bit time-modulated reflectarray for
- [15] X. Cao et al., "A 1-bit time-modulated reflectarray for reconfigurable-intelligent-surface applications," *IEEE Trans. Antennas Propag.*, vol. 71, no. 3, pp. 2396–2408, Mar. 2023.

BIOGRAPHIES

AHMED NASSER received the dual Ph.D. degree from Kyushu University, Fukuoka, Japan, and the Egypt Japan University of Science and Technology, Egypt, in 2020. He is currently a Post-Doctoral Fellow at the King Abdullah University of Science and Technology (KAUST).

ABDULKADIR CELIK received the Ph.D. degree in double majors of electrical engineering and computer engineering from lowa State University, Ames, IA, USA, in 2016. He is currently a Senior Research Scientist at the King Abdullah University of Science and Technology (KAUST).

ASMAA ABDALLAH received the Ph.D. degree in electrical engineering from the American University of Beirut, Beirut, Lebanon, in 2020. She is currently a Research Scientist at the King Abdulah University of Science and Technology (KAUST).

RUIQI WANG is currently pursuing the Ph.D. degree with the King Abdullah University of Science and Technology (KAUST).

YIMING YANG is currently pursuing the Ph.D. degree with the King Abdullah University of Science and Technology (KAUST).

ATIF SHAMIM received the Ph.D. degree in electrical engineering from Carleton University, Ottawa, Canada, in 2009. He is currently a Full Professor with the King Abdullah University of Science and Technology (KAUST).

AHMED M. ELTAWIL (ahmed.eltawil@kaust.edu.sa) received the Ph.D. degree in electrical engineering from the University of California at Los Angeles, Los Angeles, CA, USA, in 2003. He is currently a Full Professor with the King Abdullah University of Science and Technology (KAUST).